International Geology Review

ISSN: 0020-6814 (Print) 1938-2839 (Online) Journal homepage: http://www.tandfonline.com/loi/tigr20

Tangled up in folds: tectonic significance of superimposed folding at the core of the Central Iberian curve (West Iberia)

Daniel Pastor-Galán, Ícaro Fróis Dias da Silva, Thomas Groenewegen & Wout Krijgsman

To cite this article: Daniel Pastor-Galán, Ícaro Fróis Dias da Silva, Thomas Groenewegen & Wout Krijgsman (2018): Tangled up in folds: tectonic significance of superimposed folding at the core of the Central Iberian curve (West Iberia), International Geology Review, DOI: 10.1080/00206814.2017.1422443

To link to this article: https://doi.org/10.1080/00206814.2017.1422443

INTERNATIONAL GEOLOGY REVIEW, 2018
https://doi.org/10.1080/00206814.2017.1422443

Taylor & Francis
Taylor & Francis Group

ARTICLE

Tangled up in folds: tectonic significance of superimposed folding at the core of the Central Iberian curve (West Iberia)

Daniel Pastor-Galán[a*], Ícaro Fróis Dias da Silva[b], Thomas Groenewegen[a] and Wout Krijgsman[a]

[a]Departement of Earth Sciences, Utrecht University, Utrecht, The Netherlands; [b]Faculdade de Ciências da Universidade de Lisboa, Instituto Dom Luiz, Lisboa, Portugal

ABSTRACT
The amalgamation of Pangea during the Carboniferous produced a winding mountain belt: the Variscan orogen of West Europe. In the Iberian Peninsula, this tortuous geometry is dominated by two major structures: the Cantabrian Orocline, to the north, and the Central Iberian curve (CIC) to the south. Here, we perform a detailed structural analysis of an area within the core of the CIC. This core was intensively deformed resulting in a corrugated superimposed folding pattern. We have identified three different phases of deformation that can be linked to regional Variscan deformation phases. The main collisional event produced upright to moderately inclined cylindrical folds with an associated axial planar cleavage. These folds were subsequently folded during extensional collapse, in which a second fold system with subhorizontal axes and an intense subhorizontal cleavage formed. Finally, during the formation of the Cantabrian Orocline, a third folding event refolded the two previous fold systems. This later phase formed upright open folds with fold axis trending 100° to 130°, a crenulation cleavage and brittle–ductile transcurrent conjugated shearing. Our results show that the first and last deformation phases are close to coaxial, which does not allow the CIC to be formed as a product of vertical axis rotations, i.e. an orocline. The origin of the curvature in Central Iberia, if a single process, had to be coeval or previous to the first deformation phase.

ARTICLE HISTORY
Received 23 August 2017
Accepted 26 December 2017

KEYWORDS
Iberia; Central Iberian curve; orocline; superimposed folding; Variscan

1. Introduction

Orogens represent the most astonishing outcome of plate tectonics. They control the growth of continental crust, influence the local – and sometimes global – climate, and host the bulk of Earth's resources. Among the structures formed during orogenesis, folds are visually attractive: nothing as impressive as a solid rock buckled as modelling clay in your hand. Folds form from microscale to lithospheric scale (Cloetingh *et al*. 2002; Pastor-Galan *et al*. 2012a) and their geometry and expression carry crucial information about deformation mechanisms and tectonics of the area. In many orogens, the earliest fold generations have been refolded as the result of overlapping deformation phases after mountain belt growth and collapse. Unravelling the deformation history is crucial to understand the tectonic and geodynamic evolution of any orogen and, consequently, the operating processes during rock deformation.

The largest scale folds on Earth are known as oroclines, which are the result of buckling or bending an originally linear orogen or a crustal fragment (Pastor-Galán *et al*. 2017). Oroclines can affect from the upper crust to the entire lithosphere (Pastor-Galán *et al*. 2017 and references therein). The process of orocline bending or buckling produces contrasting effects in oroclines' limbs and hinges. Orocline limbs show the larger vertical axis rotations (Meijers *et al*. 2017; Pastor-Galán *et al*. 2017; van der Boon *et al*. 2018), coaxial deformation, and orogen parallel strike-slip faults (e.g. Pastor-Galán *et al*. 2014; Gutiérrez-Alonso *et al*. 2015; Shaw *et al*. 2016a). In contrast, orocline hinges are characterized by less significant rotations (e.g. Weil *et al*. 2013) and non-coaxial deformation (Pastor-Galán *et al*. 2012b; Li and Rosenbaum 2014) resulting in complex fold interference patterns.

The Variscan–Alleghanian orogen is a multi-episodic orogen in which several folding events produced striking interference folding patterns (e.g. Chopin *et al*. 2012). In Iberia, its trend depicts a sinuous 'S-shaped' geometry of two opposing first-order magnitude folds

CONTACT Daniel Pastor-Galán dpastorgalan@gmail.com Departement of Earth Sciences, Utrecht University, Heidelberglaan 8, Utrecht 3584 CS, The Netherlands
*Present address Center for Northeast Asian Studies, Tohoku University, 41 Kawauchi, Aoba-ku, Sendai, Miyagi, 980-8576, Japan.
The supplemental data for this article can be accessed here.

(Figure 1) delineated by the well-known Cantabrian Orocline in the north and the Central Iberian curve (CIC) to south, an alleged orocline whose geometry and kinematics are intensely debated (Figure 1; e.g. Aerden 2004; Martínez Catalán 2011; Shaw *et al*. 2012; Dias *et al*. 2016). In this paper, we explore the structure of superimposed folding patterns from the hinge zone of the CIC to test if the observed curvature was consequence of large differential vertical axis rotations during a process of orocline buckling/bending analogous to the Cantabrian Orocline.

2. Background

Closure of the Rheic Ocean and collision between Laurussia and Gondwana resulted in the Variscan–Alleghanian orogen, a major orogenic belt that formed during the amalgamation of Pangea (e.g. Nance *et al*. 2010; Stampfli *et al*. 2013; Domeier and Torsvik 2014). In the Iberian Peninsula, the first evidence of continental collision is dated at ca. 365–370 Ma (e.g. Dallmeyer and Ibarguchi 1990; Quesada 1991; Dallmeyer *et al*. 1997; Gómez Barreiro *et al*. 2006; López-Carmona *et al*. 2014) followed by several diachronic deformation phases (e.g. Díez-Balda *et al*. 1995). The Cantabrian Orocline (or Ibero-Armorican arc) formed as a late orogenic feature in a short period of ca. 10–15 million years between 310 and 295 Ma (Weil *et al*. 2010; Pastor-Galán *et al*. 2011, 2014) and is characterized by a curved structural trend that traces an arc from Brittany across the Bay of Biscay passing through south England and Ireland into the Central Iberian Zone (CIZ) (Figure 1; Pastor-Galán *et al*. 2015a). An assortment of palaeomagnetic and geological data supports secondary oroclinal kinematics, i.e. an originally near-linear Variscan orogenic edifice buckled around a vertical axis (e.g. Gutiérrez-Alonso *et al*. 2012; Weil *et al*. 2013 and references therein). The deformation phase associated with the formation of the Cantabrian Orocline resulted in strongly non-coaxial deformation in the hinge of this orocline generating a set of radial folds with conical geometry that refolded the original fold-and-thrust belt into an anastomosing interference pattern (Pastor-Galán *et al*. 2012b).

Some authors hypothesized a second orogenic bend to the south of the Cantabrian Orocline and with opposite curvature, so-called Central Iberian Orocline (also Central Iberian arc). Despite the kinematic implications of the name, most of its geometry and kinematics are still unknown (Dias *et al*. 2016; Pastor-Galán *et al*. 2016, in press; Dias da Silva *et al*. 2017), for that reason, we refer to it as 'CIC' hereafter to avoid using terms implying certain kinematics of formation. Staub (1926) hypothesized on its geometry for the first time (see Martinez Catalan *et al*. 2015 for a historical perspective). After being ignored for decades, Aerden (2004) recovered Staub's hypothesis following the structural trend of folds and inclusion trails in garnet porphyroblasts. More recently, Martínez Catalán (2011) and Shaw *et al*. (2012) suggested alternative geometries for the CIC. However, the three models share two common features: (1) the curvature runs parallel to the CIZ, located in the centre-west of Iberia, and (2) all place the Galicia-Trás-os-Montes Zone (GTMZ; Figure 1; Farias *et al*. 1987) in the core of the bend. The eastern boundary of the GTMZ with CIZ is the best exposure of the Central Iberian curvature.

Some authors have suggested that the Cantabrian Orocline and CIC buckle together as secondary oroclines (e.g. Martínez Catalán 2011; Shaw and Johnston 2016b), mostly based on aeromagnetic anomalies (Martínez-Catalán 2011) and palaeocurrent analyses (Shaw *et al*. 2012), the latter being under debate (Dias *et al*. 2016). Recent palaeomagnetic data from the hinge and southern limb of the CIC discarded a coeval formation for both orogenic curves (Pastor-Galán *et al*. 2015b, 2016, in press). Alternative hypothesis explaining the arcuate geometry of the CIC restricts such curvature the GTMZ (e.g. Ribeiro 1974) and adjacent areas the most prominent are (1) an extrusion wedge product of a non-cylindrical collision that dragged the earliest most Variscan folds (Martínez-Catalán 1990; Dias da Silva 2014); (2) a klippen of a large-scale allochthonous thrust sheet that thrusted most of the Palaeozoic rocks of Iberia (Rubio Pascual *et al*. 2013, 2016; Martinez Catalan *et al*. 2014; Díez Fernández and Arenas 2015); (3) the relic of a narrow seaway formed at the Late Devonian during the early stages of the Variscan orogeny (Dias *et al*. 2016).

3. Geological setting

In the eastern rim of the Morais Allochthonous Complex (Figures 1 and 2), two tectono-stratigraphic domains are juxtaposed: the GTMZ and the CIZ. The GTMZ (Farias *et al*. 1987), structurally higher, is composed by far-travelled allochthonous units including oceanic and continental rocks stacked in the Variscan accretionary prism. The units thrusted the Iberian autochthon eastward (present coordinates) at 400–370 Ma (Ribeiro 1974; Ribeiro *et al*. 1990; Gómez Barreiro *et al*. 2007; Rodrigues *et al*. 2013; Dias da Silva 2014). The allochthonous units used the 'Parautochthon' (also referred as 'Schistose Domain'; Farias *et al*. 1987) as the main detachment tectonic sheet (Dias da Silva *et al*. 2014, 2015a, 2015b).

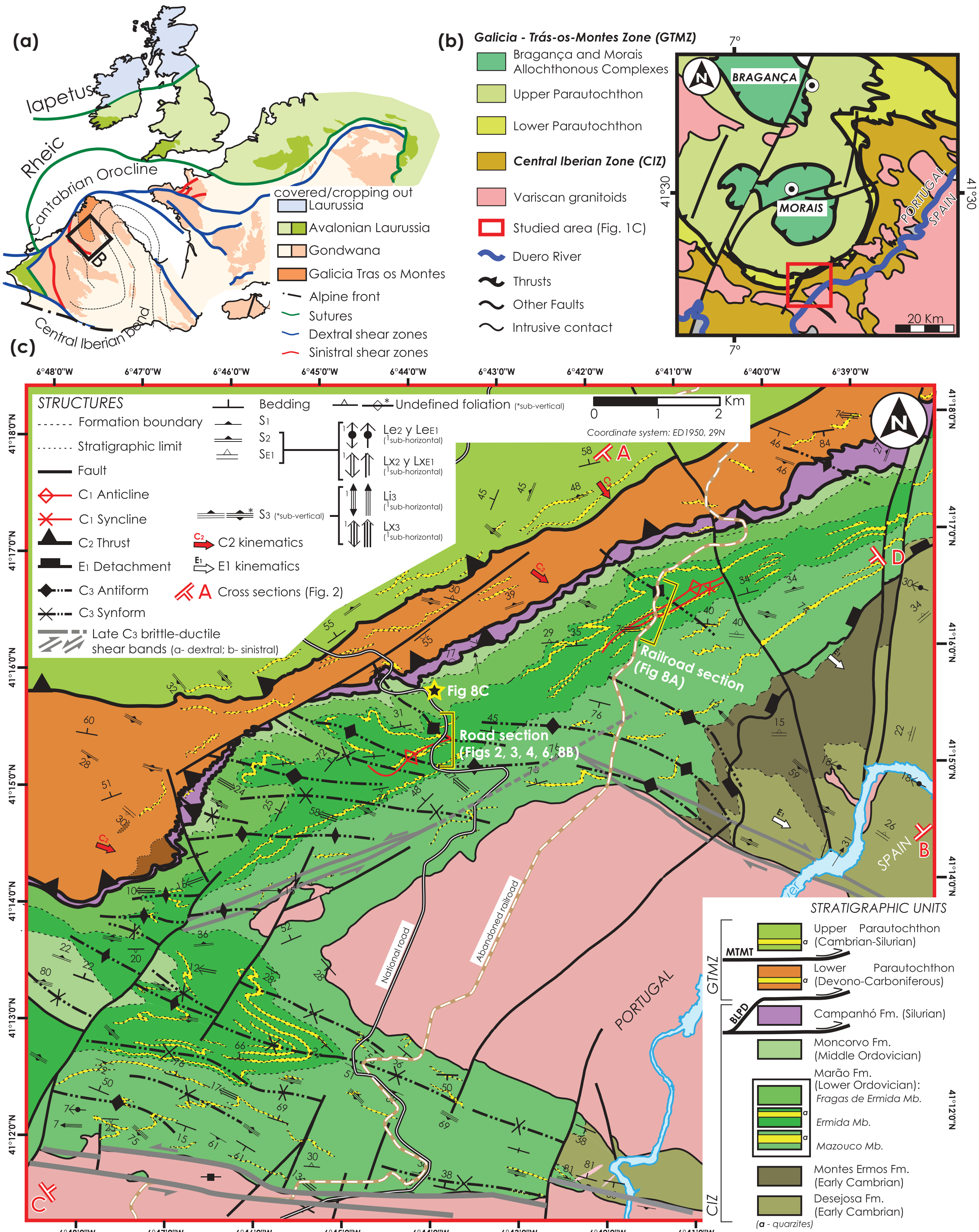

Figure 1. (a) Terrain map of the Variscan orogen of western Europe showing the Cantabrian Orocline and Central Iberian curve. (b) General geology in the surroundings of the Morais Complex. The square marks the study area. (c) Geological map of the study area. It shows the major structures following the code in Dias da Silva (2014). See Supplementary Table 1. Dashed grey line marks the possible prolongation of the sinistral shear band as proposed by Dias (1986), which may explain the trend variation of the C_3 fold axes.

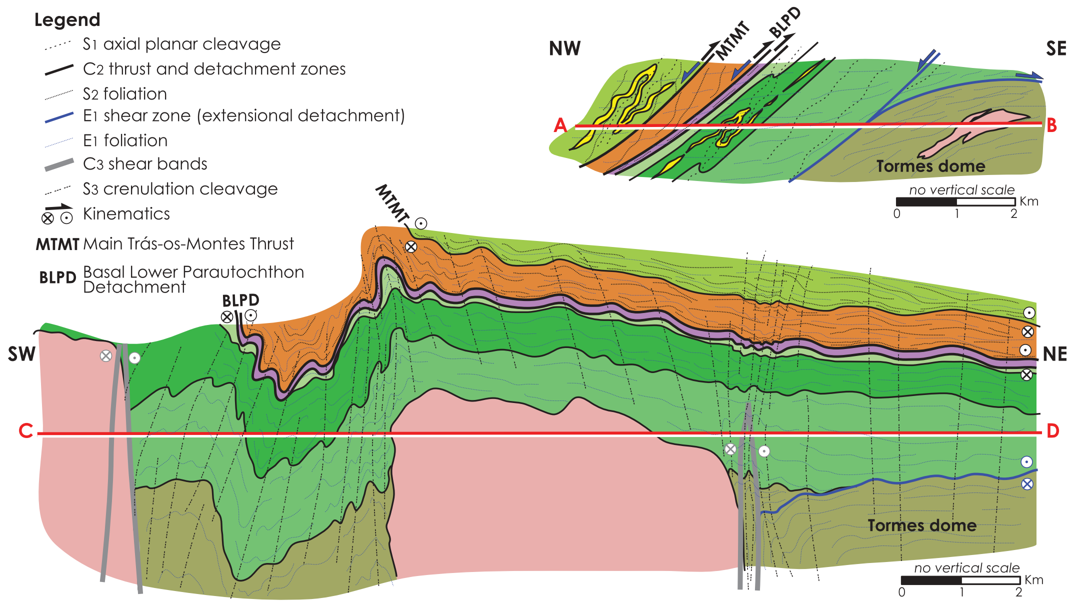

Figure 2. General cross sections perpendicular to the trend of the Central Iberian curve (a,b) and perpendicular to D_3 folds (b,c).

The CIZ is the autochthonous domain and contains a late Neoproterozoic/lower Cambrian to Carboniferous stratigraphic record, including Cambro-Ordovician magmatic rocks, deposited in the northcentral Gondwana passive margin during the opening of the Rheic Ocean (e.g. Gutiérrez-Marco *et al*. 1990; Valladares *et al*. 2000). Both the CIZ and the Parautochthon were affected by polyphase deformation under very-low to high-temperature metamorphic conditions during the Variscan orogeny.

The first deformation stage (D_1) produced two events (C_1 and C_2, after Dias da Silva 2014; Martinez Catalan *et al*. 2014; Supplementary Table 1). C_1 occurred ~360 Ma (Dallmeyer *et al*. 1997) and produced steep axial planar cleavage folding. C_1 folds in the eastern rim of the Morais Allochthonous Complex have a general centrifuge vergency in respect to the allochthonous core first described by Ribeiro (1974), showing a mainland propagation of the orogenic front, from the Parautochthon to the CIZ (Dallmeyer *et al*. 1997). The C_1 was thrusted and detached after a subsequent compressive phase (C_2), dated at ~340 Ma (Dallmeyer *et al.* 1997), responsible for the stacking of the parautochthonous units over the CIZ (Figures 1 and 2). C_2 deformation provoked a retightening and an increase of the C_1 fold headings, with parallelization of the fold axis and planes to the main low-dipping shear zones (Pereira 1987; González Clavijo 2006; Rodrigues *et al*. 2013; Dias da Silva 2014). A pervasive greenschist facies crenulation cleavage developed especially along the more phylonitic bands as in the Main Trás-os-Montes Thrust (MTMT) and Basal Lower Parautochthon Detachment (BLPD; Figure 1). The C_2 foliation is almost restricted to the GTMZ rocks, being only represented in the CIZ by the BLPD, which used the Silurian carbonaceous slates as a preferred sliding plane to tectonically carry the lower and the upper Parautochthon onto the autochthon (Figures 1 and 2; Dias da Silva 2014; Martinez Catalan *et al*. 2014 and references within).

Overburden triggered syn-orogenic extensional collapse and related isostatic rebound of deep settled crust at ~330–320 Ma (e.g. Escuder Viruete *et al*. 1994; Rubio Pascual *et al*. 2013). The first extensional event (D_2 after; Díez-Balda *et al*. 1995; E_1 after Martinez Catalan *et al*. 2014; Supplementary Table 1) led to the formation of extensional domes, anatectic melting, and emplacement of syn- to post-D_2 granitic bodies (e.g. López-Moro *et al*. 2012). During extension, a flat-lying foliation (Figures 2 and 3) developed pervasively (e.g. Escuder Viruete *et al*. 1994). The lack of conclusive shear-sense criteria in the foliation has been interpreted as the change of the tectonic regime from simple to pure-shear deformation towards the upper structural levels, away from the main detachment zones (Dias da Silva 2014).

A late Variscan deformation phase (D_3 or C_3; Supplementary Table 1) took place at ~315–300 Ma (e.g. Díez-Balda *et al*. 1995). D_3 produced NW–SE to E–W heterogeneous folding, with sub-horizontal axis and fan-like disposition of their planes (e.g. Alonso and Rodríguez Fernández 1981). Towards the deeper structural levels and in more granitic areas, late-C_3 brittle–ductile conjugated shear bands accommodated the final shortening of the Variscan compressive pulse in

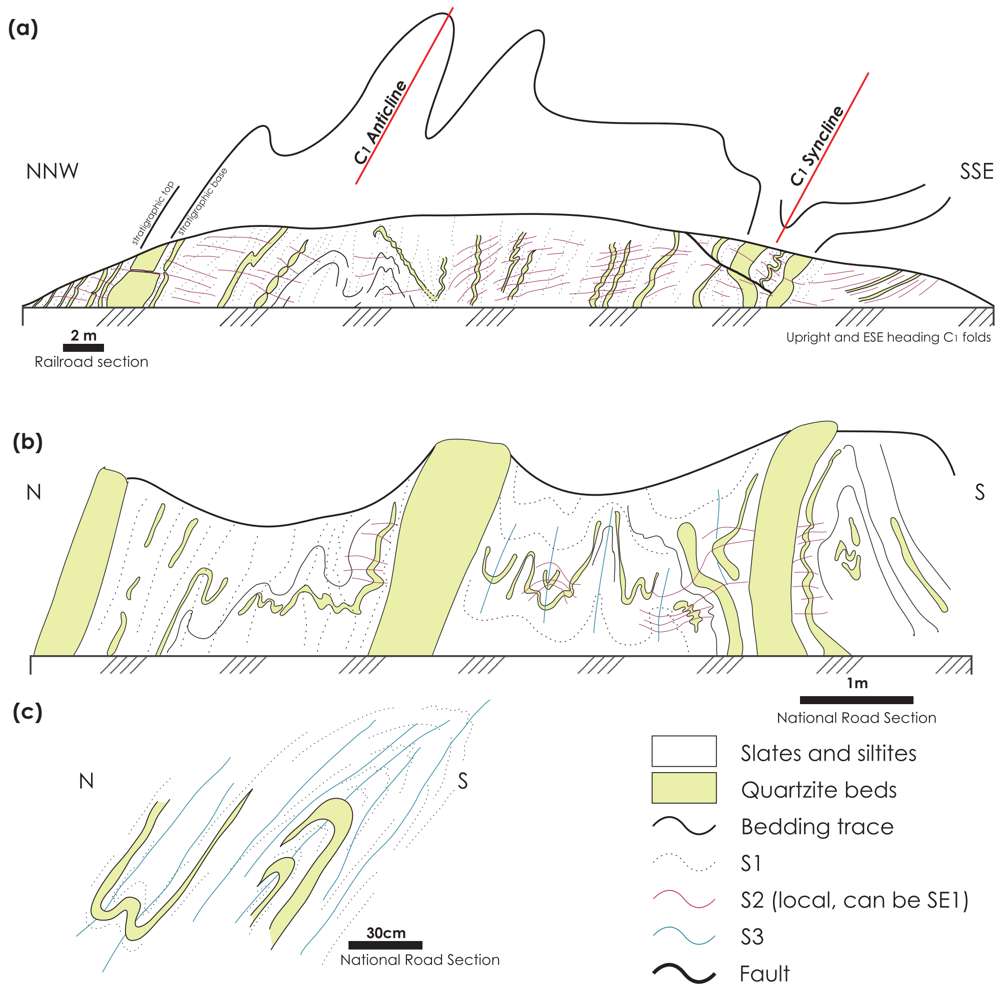

Figure 3. Field sections showing the main field relationships between structures. (a) Drawing coming from an abandoned railroad close to the Mogadouro road section (UTM-ED1950, 29°N; *X*: 693,690, *Y*: 4571,695). In some parts of the section, S_1 is be oblique to S_0. We interpret that feature as the fan like effect of the cleavage in antiforms and synforms and by rheological contrast between quartzite and pelite beds. (b) Piece of the Mogadouro road section (*X*: 690,131, *Y*: 4569,460). (c) Detailed field relations from the Mogadouro road section.

Iberia (Gutiérrez-Alonso *et al*. 2015). During this stage, large and voluminous granitic magmatism affected the autochthon, which has been interpreted as a product of lithospheric delamination triggered by oroclinal buckling (Gutiérrez-Alonso *et al*. 2004, 2011a, 2011b).

4. Macrostructure of the hinge zone of the CIC

We have constructed a detailed geological map of the study area, east of the Morais Complex (Figure 1(c); data extracted from Dias da Silva 2014), collected in total more than 1000 field measurements and identified three deformation phases. The oldest structures (D_1) include E–W to NE–SW-striking showing axial-planar low-grade cleavage (S_1, this work). Due to the tight folding recorded in the area, S_1 (Figures 1(c) and 2) is often sub-parallel to the bedding (S_0, Figures 3 and 4). D_1 folds often appear as fish-hook interference folds with waving limbs and variably dipping hinges but they gently head southeast and follow the trend of the D_1 thrusts and detachments that define GTMZ–CIZ boundary (Figures 1(c), 2, 3, 5, and 6).

The second deformation phase (D_2) was responsible for the formation of extensional detachments that bound dome-shaped structures where deep-settled hot crust was exhumed into upper structural realms (Figures 1 and 2). The major D_2 structure is defined as 'Tormes Dome' (Figure 2; e.g. López-Moro *et al*. 2012). D_2 formed a subhorizontal cleavage (S_2 in this paper) that was subsequently folded by D_3 (Figure 4(c)) and frequently includes a WNW–ESE-stretching lineation and top-to-east-southeast shear criteria (Figures 1–9; e.g. Escuder Viruete *et al*. 1994; Dias da Silva 2014).

A pervasive subhorizontal crenulation cleavage (S_2) developed in the uppermost slate unit (Figures 2 and 4 (c)), including the entire Parautochthon, showing that

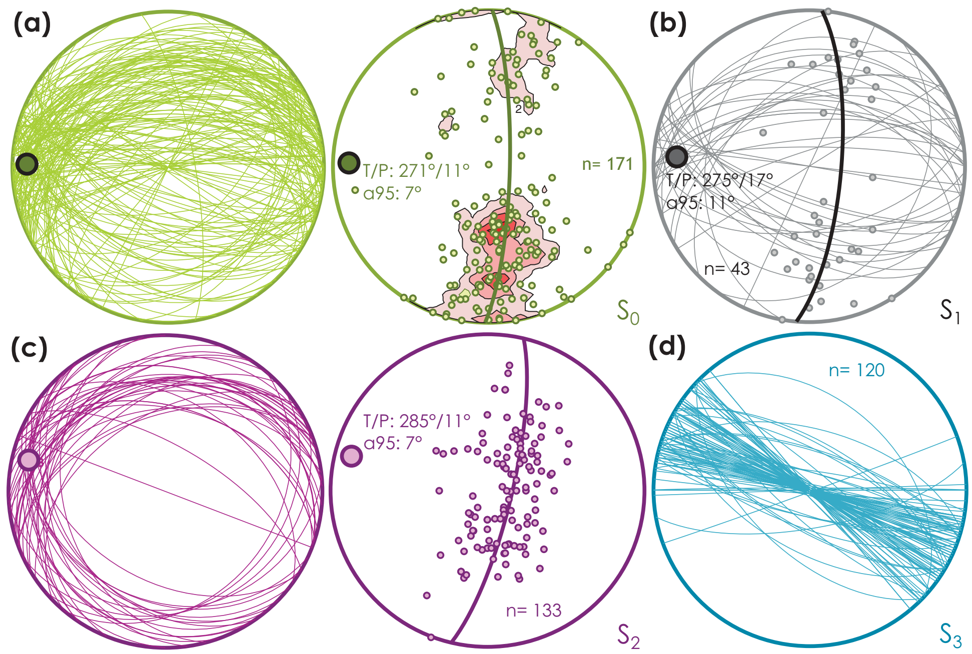

Figure 4. Stereonet analysis of the data compiled in the area. (a) S_0 planes (left) and poles to planes with 2% contours (right). T/P indicates the trend and plunge of the best cylindrical fit, which is a combination of the three different phases of deformation. (b) Planes and pole to the planes of S_1. T/P is a combination of D_2 and D_3. (c) Planes and poles to the planes of S_2. Note that the cleavage is folded as a result of D_3. (d) Orientation of S_3.

D_2 also affected the higher structural realms where the metamorphism only reached the chlorite zone. As response to the thermal uplift in the Tormes Dome, the main D_1 (C_2) thrusts and detachments (MTMT and BLPD) were verticalized and reactivated with top-to-west-northwest shear sense, allowing the regression of the GTMZ. C1 folds were parallelized to the lowermost extensional shear zones and witnessed vertical axis rotations towards the extensional shear-band trend (NE–SW, Figure 1(c)). These early folds were vertically flattened producing the waving of their axial planes and limbs (Figure 2; Dias da Silva 2014).

The youngest phase (D_3) produced gentle to tight folds with variable plunging axes which we could characterize using the originally subhorizontal S_2 (mean trend/plunge of 285°/11°; Figure 4(c)). This deformation event generated a set of brittle–ductile transcurrent-shear zones that cut syn-D3 granitoids and transpose the earlier fabrics (Figure 1(c); e.g. González Clavijo and Díez Montes 2008). The D_3 folds and axial planar cleavage (S_3; Figures 1(c)–4) show vertical and horizontal fan-like arrays, with trends from E–W to NW–SE and axial plane dips between 70° (NE and SW) and 90° (Figures 1(c) and 2). This dispersion shows that the D_3 folding was constrained by a previous crustal structure and that these folds were locally dragged and parallelized to the late-D_3 shear zones. The plunging variation of the D_3 axes from nearly subhorizontal to subvertical and from northwest to southeast is mainly due to the interference of precursory structures (D_1 and/or D_2 folds and shear zones) and we can assume a regional sub-horizontal disposition of the D_3 folding axis.

5. Structural analysis of the Mogadouro road section: geometry and timing

We have studied the Mogadouro road section, an excellent road outcrop in Portugal, to better constrain the observed structural relations of the region. The Mogadouro road section (road code: N221) is located to the southwest of the Morais complex (GPS coordinates: 41.25212°N, 6.73172°W; Figure 1). The section is about 40 m long and the exposure is continuous at both sides of the road. The outcrop shows an Early Ordovician multilayer consisting in quartzitic and pelitic layers of varying thickness and lateral extent (Figure 1; Marão Formation). The section contains folds, mullions, and foliations that have been subsequently refolded (Figures 5–7). In this section, we collected 151 bedding planes (Figure 8(a)), 78 planes of tectonic foliations corresponding with S_2 (Figure 8(b)), 69 intersection lineations between S_2 and S_3 (Figure 8(c)), and 66 directly measured fold axes in mullions of which part of them are related to D_2 and others to D_3 (Figure 7(b)). We also collected 19 oriented samples to produce 24

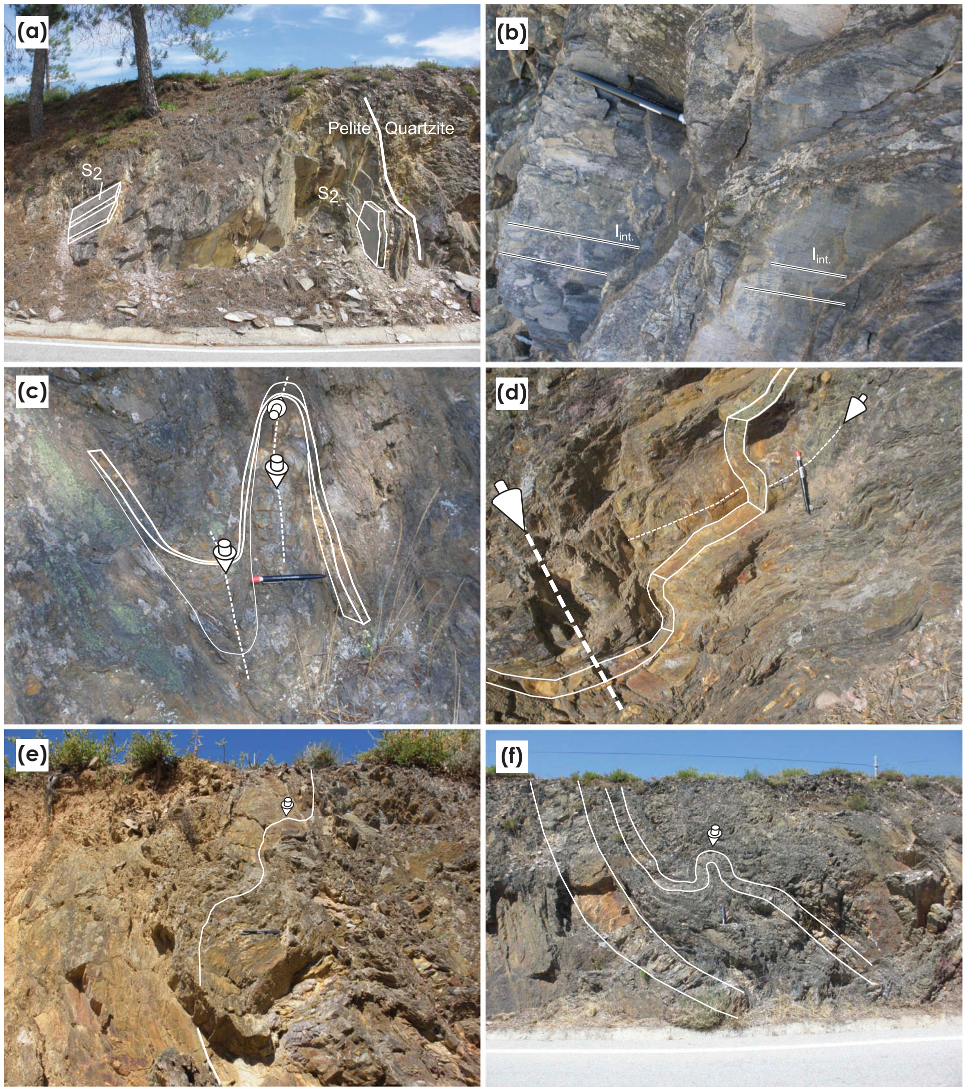

Figure 5. Field images from the Mogadouro section. Solid lines mark S_0 and dotted lines and arrows mark trend and plunge (respectively) of fold axes. (a) S_2 folded by D_3. (b) Typical look of the intersection lineation. (c) Refolded fold in quartzitic layers, note the different attitudes of the fold axes. (d) Refolded folds in quartzitic layers, again with contrasting fold axes. (e,f) Different folding styles between thick pelitic layers and the quartzitic section.

thin sections for petrographic analysis (Figure 9; Supplementary material 1). All structural data were processed using the software 'Stereonet' [Cardozo and Allmendinger 2013; we used the patch for conical folding analysis from Mulchrone *et al*. (2013)].

5.1. Mesostructure

Bedding planes (S_0) are evident only where continuous sandstone/quartzite layers are present. S_0 is strongly folded showing striking interference patterns (Figures 5 and 6). Where pelites are not interbedded with sandstone, S_0 is not obvious to the naked eye. It was not possible to discriminate the different deformation episodes based on the geometry of the bedding. When plotted in a stereonet, the poles plot along a small circle suggesting some sort of conical geometry (Figure 8(a)) possibly as a result of the interference between the phases. Geometrically, a conical fold is characterized by the trend and plunge of its axis and by the angle between the generatrix of the conical surface and the fold axis, also known as semi-apical angle ($\alpha/2$) (e.g. Pueyo *et al*. 2003). The fold axis trend/plunge is 262°/67° and its $\alpha/2$ = 72°.

Occurrence of Mullions is common in the most competent layers in the section. An exposure of an entirely folded bedding plane showing two mullion generations (Figure 7) and a piece of pelite outcrop in its core permits a detailed geometrical analysis to unravel the different deformation phases recorded by S_0. The first generation of mullions, FA_x hereafter, with

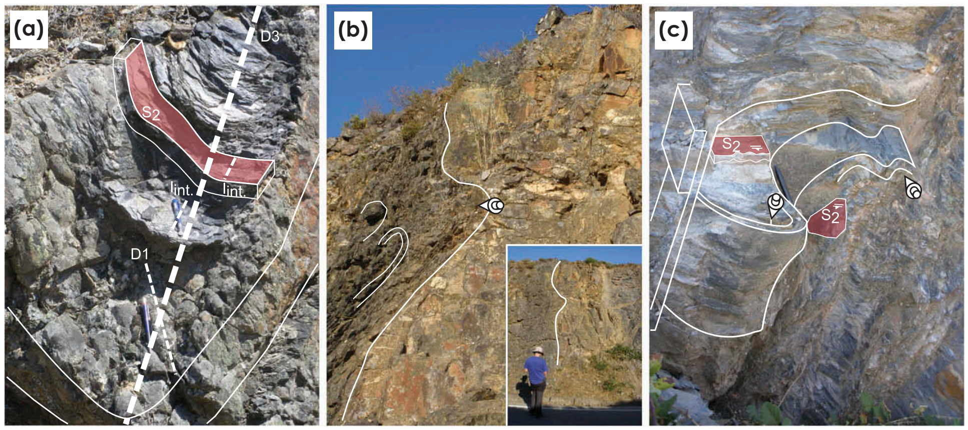

Figure 6. Field images from the Mogadouro section. Solid lines mark S_0 and dotted lines and arrows mark trend and plunge (respectively) of fold axes. (a) Effects of the D_3 deformation phase in the S_0 and S_2. Note the formation of mullions in the quartzitic layers and the different orientation of fold axes. (b) Different folding styles between thick pelitic layers and the quartzitic section. (c) Refolded fold in quartzitic layers, note the different attitudes of the fold axes.

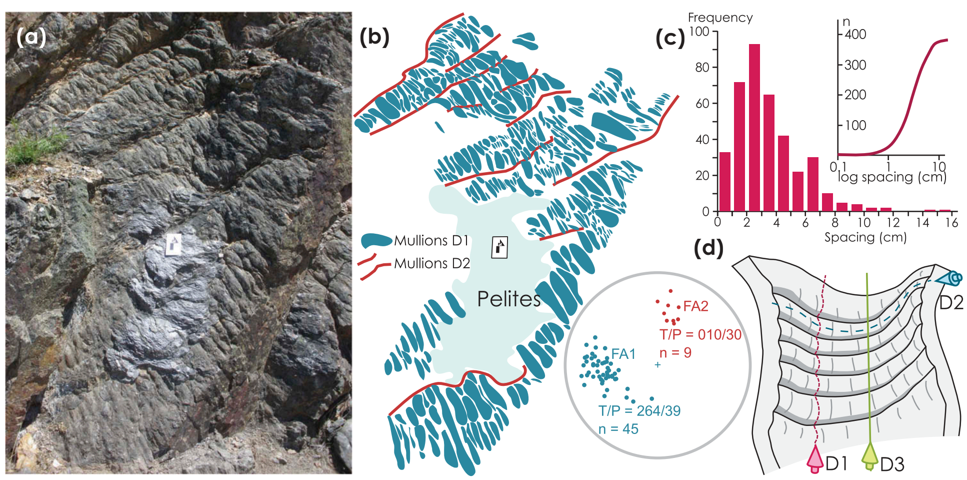

Figure 7. Structural analysis of mullions. (a) Photograph (with scale) of the bedding plane showing the mullions. (b) Photograph analysis. (c) Frequency (number of mullions) *versus* spacing. Note the skewed log-normal distribution. On the right corner is the cumulative number of mullions *versus* the log of the spacing. The straight line indicates the fractal behaviour of mullionage whereas the starting and end tips mark an undersampling of those frequencies (Pastor-Galán *et al*. 2009). (d) Interpretation of the outcrop marking the deformation phase responsible for each structure.

an average of trend/plunge = 264°/39° (Figure 7) shows an anastomosing pattern in which the continuity along its axis is inhibited by mullions of a later phase (FA_{x+1}). The space between FA_x mullions ranges from 0.1 to 15.7 cm (average 3.5 cm) and follows a log-normal distribution and fractal dimension (Figure 7(c)) as other geological features (Wu 1993; Pastor-Galán *et al*. 2009).

A second generation of mullions FA_{x+1} deformed the FA_x (Figure 7(a,d)). FA_{x+1} mullions show an average orientation 030°/10° and spacing between 17 and 39 cm (average = of 26 cm). Folds with shallow fold axes are not restricted to mullions only but are present throughout the section (Figures 5 and 6). Both FA_x and FA_{x+1} structures have been refolded by a later event. This event formed open folds with a steep fold axis (Figure 7(d)) in the quartzite layer (S_0), but shallow axis in the pelite foliation. This exposure defines three different deformation phases (D_1, D_2, and D_3). D_1 is responsible of folding (F_1) accompanied by the development of FA_x mullions (FA_1 hereafter). D_2 folded F_1 and FA_1 and produced FA_{x+1} (FA_2) and finally D_3 refolded the entire structure.

In addition to S_0, the most consistent structure in the section is a penetrative cleavage (S_x onwards). S_x is a shallow dipping cleavage, strongly developed in pelitic layers but only partially in the sandstone/quartzitic layers (Figures 5 and 6), which usually refract it

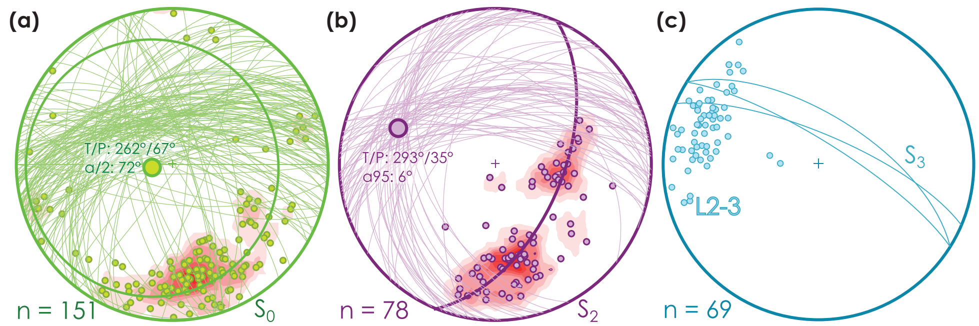

Figure 8. Stereonet of the data collected in the Mogadouro section. (a) S_0 planes and poles to planes with 2% contours (right). T/P indicates the trend and plunge of the best conical fit (following Mulchrone *et al.* 2013), which is a combination of the three different phases of deformation. (b) Planes and poles to the planes of S_2. T/P is the result of D_3. (c) Intersection lineation between S_2 and S_3 and the three only planes we could clearly identify as S_3 (*X*: 690,381, *Y*: 4569,907).

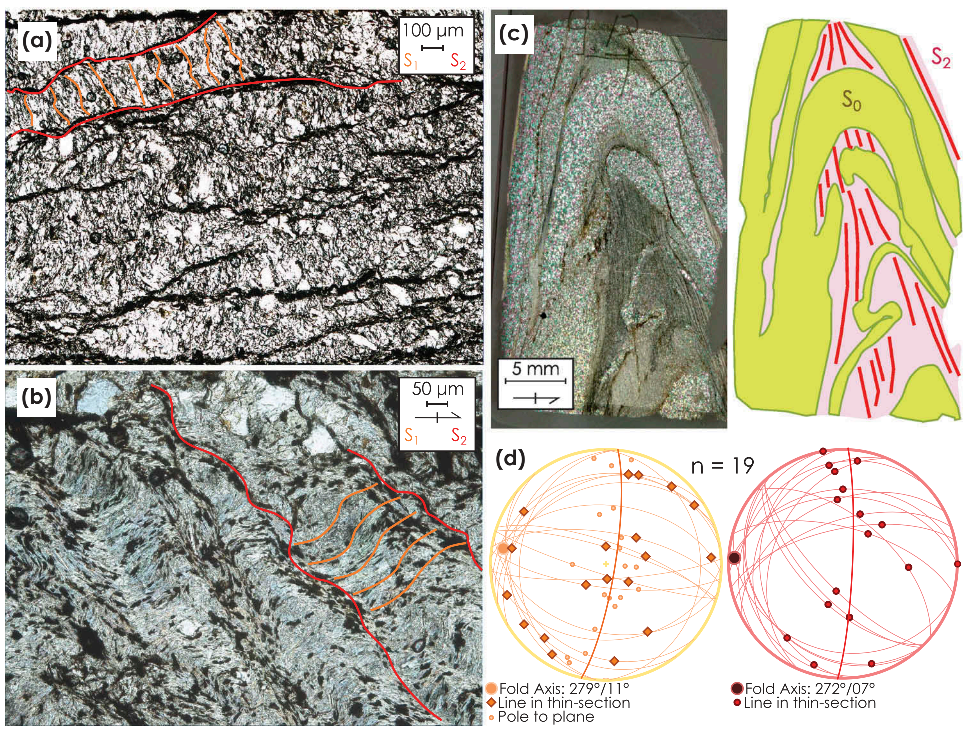

Figure 9. Thin-section analysis. (a,b) Photographs showing the relations between foliations in thin section. (c) High-resolution scan of thin section cut parallel to S_3. It shows a microfold affecting S_0, whereas the S_2 foliation is axial planar to this fold. S_0 layers are thickened in the hinge zone, while the flanks are thinned. The fold is a nice example of Ramsay folds class 2 in the quartzitic layers and 3 in the pelitic (Ramsay 1967), see also Supplementary material 1, thin-section 9B. (d) Stereonet analysis of all thin sections (see Supplementary material 1).

(Figure 6(b)). S_x strike and dip vary throughout the section. In many cases, S_x is folded, in others is axial planar to folds (Figures 5(a,c) and 6(a,c)). When plotted in a stereonet, S_x shows a mean folding axis with trend/plunge: 293°/35° (a95 = 6°). Therefore, variation in the S_x orientation can be explained by one cylindrical folding event (Figure 8(b)). In addition to S_x, another foliation comes out in areas where pelitic layers are interbedded with quartzitic strata (Figure 8). This foliation is not very penetrative and is overprinted by S_x so we will refer to it as S_{x-1}.

Another widespread structure is an intersection lineation that is visible on the S_x planes (Figures 5(b), 6(a); coded L_{int}). The orientation of these lineations forms an elongated cluster, with a mean direction of trend/plunge = 289°/23° (Figure 8(c)). Lineation is independent from S_0 and it is coincident within error with the fold axis depicted by S_x. This intersection lineation is the result of a cleavage S_{x+1} which in some cases is coincident with some axial planar foliations. Relative timing implies S_x is coeval with FA_2, since both have one event predating and one event post-dating the structures. S_{x-1} and S_x are, therefore, a product of D_1 and D_2, respectively (and will call them S_1 and S_2).

5.2. Microstructure

We collected 19 oriented samples and produced 24 thin sections for petrographic analysis (Figure 9; Supplementary material 1). All samples were cut perpendicular to the intersection lineation (labelled A when more than one section) and some of them were also cut parallel to the lineation and perpendicular to S_2 and parallel to S_2 (B and C, respectively).

All thin sections contain quartz, muscovite or chlorite, and oxides in different ratios (Figure 9; Supplementary material 1). The quartzitic domains contain less muscovite, detrital accessory minerals, and oxides, representing less than 10% of the total composition. The pelitic domains have a variable composition, containing quartz, muscovite, and oxides in varying relative amounts. Most of the thin sections show some accessory tourmaline crystals. Mineral assemblages indicate that deformation occurred under low greenschist facies.

Thin sections revealed three foliations S_0, S_1, and S_2. S_0 and S_1, always crenulated, are visible in some thin sections. S_2 is present in all the pelitic and some quartzitic domains (Figure 9; Supplementary material 1). Some thin sections show S_2 folded. In such cases, S_1 foliation is parallel to the axial plane to the latter folds (Figure 9(a, b); Supplementary material 1). Cross-cutting relations indicate three deformation events in which D_1 forms foliation S_1, a second non-coaxial deformation phase produces S_2, and a third deformation phase, D_3, forms a crenulation cleavage parallel to S_1 foliation during the folding of S_2. Thin section revealed that S_1 is folded following a fold axis with trend/plunge = 279°/11°, which is most likely a combination of D_2 and D_3 events. Likewise, S_2 shows a fold axis with trend/plunge = 294°/22° formed responding to D_3. This fold axis is statistically identical to the orientation of the fold axis determined from S_2 in the macrostructure (289°/23°).

5.3. Unravelling the orientation of D_1 fold axis

Our data analysis furthermore allows retrodeformation of the mullions outcrop, permitting to better constrain the geometry produced by each deformation phase, at least locally. Poles to S_2 show gently plunging upright folds (Figures 7 and 10). The D_3 fold axis is trend/plunge 293°/35°, similar to the axis measured in the pelites at the core of fold containing the mullions (Figure 10). When we unfold S_0 plane around the D_3 fold axis (Figures 7 and 10), we can restore the D_2 fold axis (Figure 10(a)) obtained from FA2 mullions. After restoring D_3, D_2 axes became slightly steeper with a trend/plunge = 043°/14° (originally T/P = 030°/10°). Knowing local fold axes orientations for D_3 and D_2, we can retrodeform the D_1 mullions to their original orientations (Figure 10(b)). FA_1 field orientations scatter in an elongated pattern (Figure 4) and show and average direction of 261°/39°, with a precision parameter k = 20.8 (the higher k the more precise is the data; Fisher 1953). After undoing the effects of D_3, the average orientation is 265°/35° and k = 32.3. Finally, when we unfold D_2, we find the original FA_1 trend/plunge of 295°/07°, k = 43.4. Clustering improves after each step (Figure 10(b)) and the originally elongated distribution of FA_1 transforms into a rounded and *fisherian*

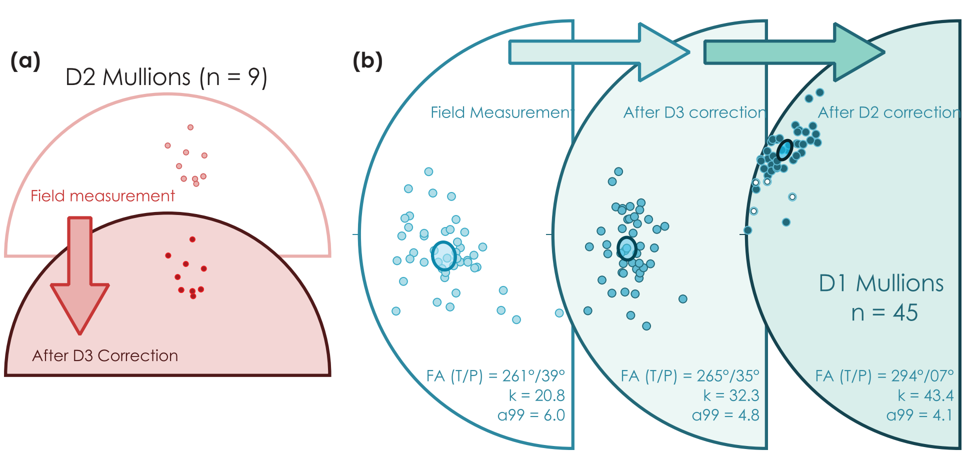

Figure 10. Result of retrodeformation of the mullions in the Mogadouro road section. (a) Unfolding the effects of D_3 on D_2 mullions. Unfolding the effects of D_3 and D_2 in D_1 mullions.

distribution around the average, a good indicator of the rightness of the correction. After correction, the strike of D_1 fold axes is identical to D_3 axes (D_1 = 295°; D_3 = 293°).

6. Tectonic significance

We have identified three different deformation and folding phases in the CIZ, in the core of the CIC, which can be linked with the regional phases described for the allochthonous and autochthonous domains of northwest Iberia (Supplementary Table 1). Figure 11 shows a cartoon synthesizing our interpretation of the deformation phases in the studied area.

6.1. Collision and collapse (D_1 and D_2)

D_1 formed originally upright to moderately inclined cylindrical folds with an associated axial planar cleavage (S_1). D_1 fold trend is varying since they were refolded by D_2 and D_3 phases (Figure 11), but the regional structure and retrodeformation of local outcrops (Figures 4 and 10, respectively) suggest an original trend ranging from 91° to 115° and subhorizontal axes. The D_1 phase observed in this region of the CIZ can be ascribed to the C_1 and C_2 stages of Dias da Silva (2014) and Martinez Catalan *et al.* (2014; Supplementary Table 1, Section 3).

D_2 deformation developed a fold system in upper slate unit with subhorizontal axes and a very penetrative subhorizontal cleavage (S_2). Structures formed in this phase were subsequently refolded by D_3 (Figure 11(c)). The orientation of D_2 structures together with the lack of simple-shear structures suggests a close to vertical shortening direction (Figure 11(b)) which we relate to a gravitational effect. We support that D_2 in the studied sections occurred synchronous with the development of extensional detachments in the Tormes Dome (see Section 3; E_1 in Supplementary Table 1) allowing the rise of its anathectic core which led to thermal enhancement of the hanging wall. Together, the combination of pure-shear and heating of the

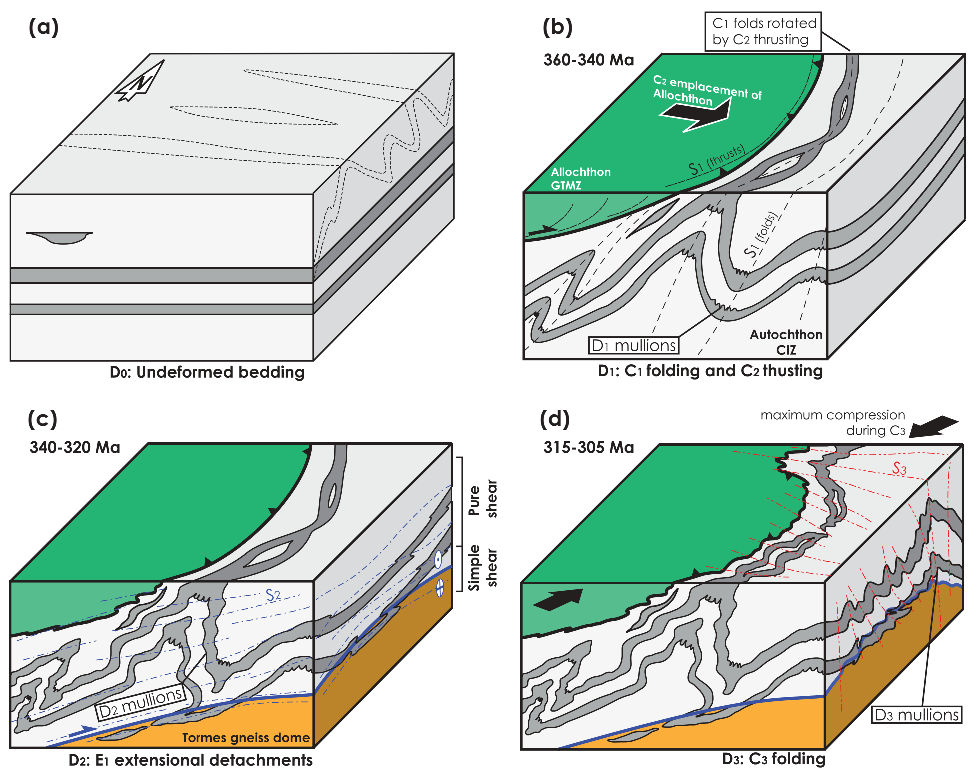

Figure 11. Cartoon showing the structural evolution in the hinge of the Central Iberian curve. (a) Undeformed stratigraphy previous to the Variscan orogeny, showing original trend of the C_1 folds (dashed line, 91°–115° directions, after complete restoration of C_3 and C_2). (b) D_1 compression: C_1 would be responsible for upright folding and development of axial planar foliation whereas the C_2 thrusting would force the centrifuge vergency around GTMZ. Mullions would form in the hinges' intrados. (c) Extensional collapse (D_2) would be responsible of close to top-down folding, mullions, and development of a very pervasive subhorizontal foliation. (d) During D_3 compressional event, the former structures refolded and the Central Iberian curve was tightened. GTMZ: Galicia-Trás-os-Montes Zone; CIZ: Central Iberian Zone.

hanging-wall block favoured the formation of a highly pervasive flat-lying crenulation cleavage (S_2 or S_{E1}; Supplementary Table 1) and axial planar centimetre to metre-scale sub-horizontal folds (Dias da Silva 2014).

6.2. Late compression (D_3)

The characteristics of D_3, fan-like dispersion of upright and slightly vergent open folding with fold axis trending 100° to 130°, the development of a crenulation cleavage (S_3), and brittle–ductile transcurrent conjugated shearing, fully coincide with those of the regional scale C_3 fabrics (Supplementary Table 1; Figures 1(c) and 2; e.g. Díez-Balda *et al*. 1995; Dias da Silva 2014; Gutiérrez-Alonso *et al*. 2015). The D_3 fold pattern adapts to the previous structure and the granitic plutons, being deflected by late-D_3 brittle–ductile shear zones (Figures 1 and 2). The obliquity with C_1 folds produced the waving of their axes, changing the plunging dramatically from sub-horizontal to near-vertical, forcing the formation of fish-hook type of folds (Figure 11). Structural analysis revealed that locally D_1 and D_3 fold axes have similar directions/trends suggesting that D_1 and D_3 deformation were close to coaxial. Its interference with C_2 thrusts and E_1 extensional regime caused the very complex fold patterns described in this paper (Figure 11(b–d)).

Palaeomagnetic data in the hinge and southern limb of the Central Iberia bend show consistent late Carboniferous counter clockwise rotations (Pastor-Galán *et al*. 2015b, 2016, in press). These rotations indicate that the full CIC was part of the southern limb of the Cantabrian Orocline during D_3. This observation does not allow the formation of the CIC after D_2, in contrast to what was proposed by several authors (Martínez Catalán 2011; Shaw *et al*. 2012, 2014; Weil *et al*. 2013; Martinez Catalan *et al*. 2014; Shaw and Johnston 2016b). Although the Central Iberian orocline could still formed as a product of vertical axis rotations (orocline) during D_1 or D_2. If the CIC was an orocline, it should have revealed an interference pattern of deformation phases resulting from a change in the stress field, i.e. strongly non-coaxial deformation. Our data support that D_1 (C_1) and D_3 (C_3) folding are close to coaxial, being D_2 (E_1) the only non-coaxial deformation phase in the studied sections. However, the vertical strain associated with D_2 is incompatible with differential vertical axis rotations. We support D_3 to be related with the formation of the Cantabrian Orocline and to the tightening of the CIC located in the southern branch of this major bend. Therefore, the CIC cannot be the result of single process of orocline buckling or bending.

The CIC, if the product of a single process, has to be either an early collisional feature. It is widely accepted that the Morais Complex is a klippen of the GTMZ allochthonous nappe complex. This fact would explain at the same time the strongly curved shape of the Morais Complex, the coaxiality of the different phases, and the coherent behaviour of the whole unit with the Southern limb of the Cantabrian Orocline. Considering the general low metamorphic grade in the studied and surrounding areas (e.g. Díez-Balda *et al*. 1995), we do not think that a larger and thick allochthonous unit could have thrusted the studied area and most of Iberia as suggested by Rubio Pascual *et al*. (2013) or Díez Fernández and Arenas (2015). A straightforward explanation, although somewhat speculative with the available data, could be that the allochtonous complexes are the relic of an extrusion wedge (Dias da Silva 2014) product of a corner effect and/or indentation of a promontory in the Gondwanan coast (e.g. Murphy *et al*. 2016), which would have been considerably shorter and thinner, thus producing a short residence time inhibiting the stabilization of the regional metamorphic isograds. The alleged promontory could have formed after an extensional episode that likely produce a small oceanic basin (e.g. Dias *et al*. 2016) recorded in the Gondwanan margin just before the continent–continent collision (Gutiérrez-Alonso *et al*. 2008).

7. Concluding remarks

We have performed detailed field and structural analyses around the hinge of the CIC (western Iberia). We have identified three different phases of deformation that can be linked to regional deformation phases of the Variscan orogeny:

- D_1 developed upright to moderately inclined cylindrical folds with an associated axial planar cleavage (S_1). D_2 deformation developed a fold system with subhorizontal axes and a very penetrative subhorizontal cleavage (S_2). We interpret D_2 to be linked with regional extensional collapse.
- D_3 is a late Variscan (315–300 Ma) compressional phase that formed upright open folds with fold axis trending 100° to 130°, a crenulation cleavage (S3) and brittle–ductile transcurrent conjugated shearing.
- D_1 and D_3 are close to coaxial. Timing and deformation style suggests that D_3 folds developed in response to the same process that formed the Cantabrian Orocline, from which the studied area represents the southern limb. Coaxiality between

D_1 and D_3 does not permit the core of the CIC to be the result of large-scale vertical axis rotations. The geometry of the CIC in the Galicia-Trás-os-Montes and adjacent areas, if a single process, is not related with large differential vertical axis rotations and had to be coeval to D_1, with D_3 responsible by its final tightening.

Acknowledgements

DPG is funded by an ISES grant and a JSPS fellowship (JP16P16329). IFDS acknowledges the financial support of the Instituto Geológico y Minero de España through its scholarship programme and the Fundação para a Ciência e a Tecnologia postdoctoral grant: SFRH/BPD/99550/2014. Reviews by K.F. Mulchrone, R. Dias, and an anonymous reviewer greatly improved the paper. This work is a contribution to project IGCP project 648 (Supercontinent Cycle and Global Geodynamics) and to IDL Research Group 4 (Continents, Islands, and Mantle). DPG would like to thank Bob Dylan for inspiration, keep on playing it "fucking loud"!

Disclosure statement

No potential conflict of interest was reported by the authors.

Funding

This work was supported by the Japan Society for the Promotion of Science: [Grant Number JP16F16329].

References

Aerden, D., 2004, Correlating deformation in Variscan NW-Iberia using porphyroblasts; implications for the Ibero-Armorican Arc: Journal of Structural Geology, v. 26, p. 177–196. doi:10.1016/S0191-8141(03)00070-1

Alonso, J.L., and Rodríguez Fernández, L.R., 1981, Aportaciones al conocimiento de la estructura del Sinclinorio de Verin: Cuadernos Xeolóxicos de Laxe, v. 9, p. 3–122.

Cardozo, N., and Allmendinger, R.W., 2013, Spherical projections with OSXStereonet: Computational Geoscience, v. 51, p. 193–205. doi:10.1016/j.cageo.2012.07.021

Chopin, F., Schulmann, K., Skrzypek, E., Lehmann, J., Dujardin, J.R., Martelat, J.E., Lexa, O., Corsini, M., Edel, J.B., Štípská, P., and Pitra, P., 2012, Crustal influx, indentation, ductile thinning and gravity redistribution in a continental wedge: Building a Moldanubian mantled gneiss dome with underthrust Saxothuringian material (European Variscan belt): Tectonics, v. 31. doi:10.1029/2011TC002951

Cloetingh, S., Burov, E., Beekman, F., Andeweg, B., Andriessen, P.A.M., Garcia-Castellanos, D., de Vicente, G., and Vegas, R., 2002, Lithospheric folding in Iberia: Tectonics, v. 21, p. 26. doi:10.1029/2001TC901031

Dallmeyer, R.D., Catalán, J.R.M., Arenas, R., Gil Ibarguchi, J.I., Gutiérrez-Alonso, G., Farias, P., Bastida, F., and Aller, J., 1997, Diachronous Variscan tectonothermal activity in the NW Iberian Massif: Evidence from 40Ar/39Ar dating of regional fabrics: Tectonophysics, v. 277, p. 307–337. doi:10.1016/S0040-1951(97)00035-8

Dallmeyer, R.D., and Ibarguchi, J.I.G., 1990, Age of amphibolitic metamorphism in the ophiolitic unit of the Morais Allochthon (PORTUGAL) - implications for early hercynian orogenesis in the Iberian Massif: Journal Geological Social London, v. 147, p. 873–878. doi:10.1144/gsjgs.147.5.0873

Dias da Silva, Í., 2014, Geología de las Zonas Centro Ibérica y Galicia – Trás-os-Montes en la parte oriental del Complejo de Morais, Portugal/España: Coruña, Instituto Universitario de Geología "Isidro Parga Pondal" - Área de Xeoloxía e Minería do Seminario de Estudos Galegos.

Dias da Silva, Í., Díez Fernández, R., Díez-Montes, A., González Clavijo, E., and Foster, D.A., 2015a, Magmatic evolution in the N-Gondwana margin related to the opening of the Rheic Ocean—Evidence from the Upper Parautochthon of the Galicia-Trás-os-Montes Zone and from the Central Iberian Zone (NW Iberian Massif): International Journal of Earth Sciences, p. 1–25. doi:10.1007/s00531-015-1232-9

Dias da Silva, Í., Gómez-Barreiro, J., Martínez Catalán, J.R., Ayarza, P., Pohl, J., and Martínez, E., 2017, Structural and microstructural analysis of the Retortillo Syncline (Variscan belt, Central Iberia). Implications for the Central Iberian Orocline: Tectonophysics, v. 717, p. 99–115. doi:10.1016/j.tecto.2017.07.015

Dias da Silva, Í., Linnemann, U., Hofmann, M., González-Clavijo, E., Díez-Montes, A., and Martínez Catalán, J.R., 2015b, Detrital zircon and tectonostratigraphy of the Parautochthon under the Morais Complex (NE Portugal): Implications for the Variscan accretionary history of the Iberian Massif: Journal of the Geological Society, v. 172, p. 45–61. doi:10.1144/jgs2014-005

Dias da Silva, Í., Valverde-Vaquero, P., González-Clavijo, E., Díez-Montes, A., and Martínez Catalán, J.R., 2014, Structural and stratigraphical significance of U–Pb ages from the Mora and Saldanha volcanic complexes (NE Portugal, Iberian Variscides): Geological Society, London, Special Publications, Vol. 405, p. 115–135. doi:10.1144/sp405.3

Dias, R., 1986, Estudo de um sector do autóctone de Trás-os-Montes oriental a ENE de Torre de Moncorvo, Lisboa: Universidade de Lisboa, p. 153.

Dias, R., Ribeiro, A., Romão, J., Coke, C., and Moreira, N., 2016, A review of the arcuate structures in the Iberian Variscides; constraints and genetic models: Tectonophysics, v. 681, p. 170–194. doi:10.1016/j.tecto.2016.04.011

Díez Fernández, R., and Arenas, R., 2015, The Late Devonian Variscan suture of the Iberian Massif: A correlation of high-pressure belts in NW and SW Iberia: Tectonophysics, v. 654, p. 96–100. doi:10.1016/j.tecto.2015.05.001

Díez-Balda, M.A., Martínez-Catalan, J.R., and Arribas, P.A., 1995, Syn-collisional extensional collapse parallel to the orogenic trend in a domain of steep tectonics: The Salamanca Detachment Zone (Central Iberian Zone, Spain): Journal Structureal Geological, v. 17, p. 163–182. doi:10.1016/0191-8141(94)E0042-W

Domeier, M., and Torsvik, T.H., 2014, Plate tectonics in the late Paleozoic: Geosci Frontiers, v. 5, p. 303–350. doi:10.1016/j.gsf.2014.01.002

Escuder Viruete, J., Arenas, R., and Martínez Catalán, J.R., 1994, Tectonothermal evolution associated with Variscan crustal extension, in the Tormes Gneiss dome (NW Salamanca, Iberian Massif, Spain): Tectonophysics, v. 238, p. 1–22.

Farias, P., Gallastegui, G., González-Lodeiro, F., Marquínez, J., Martín Parra, L.M., Martínez Catalán, J.R., de Pablo Maciá, J. G., and Rodríguez Fernández, L.R., 1987, Aportaciones al conocimiento de la litoestratigrafía y estructura de Galicia Central: Memórias da Faculdade de Ciências da Universidade do Porto, v. 1, p. 411–431.

Fisher, R., 1953, Dispersion on a Sphere: Proceedings R Social A Mathematical Physical Engineering Sciences, v. 217, p. 295–305. doi:10.1098/rspa.1953.0064

Gómez Barreiro, J., Martínez Catalán, J.R., Arenas, R., Castiñeiras, P., Abati, J., Díaz García, F., and Wijbrans, J.R., 2007, Tectonic evolution of the upper allochtonon of the Órdenes complex (Northwestern Iberian Massif): Structural constraints to a poligenic peri-Gondwanan terrane: Geologic Society of America - Special Paper, v. 423, p. 315–332.

Gómez Barreiro, J.G., Wijbrans, J.R., Castineiras, P., Catalan, J.R. M., Arenas, R., Garcia, F.D., and Abati, J., 2006, Ar-40/Ar-39 laserprobe dating of mylonitic fabrics in a polyorogenic terrane of NW Iberia: Journal Geological Social London, v. 163, p. 61–73. doi:10.1144/0016-764905-012

González Clavijo, E., 2006, La Geología del sinforme de Alcañices, *in* De Zamora, O., ed., Instituto Universitario de Geología "Isidro Parga Pongal" - Área de Xeoloxía e Minería do Seminario de Estudos Galegos: La Coruña.

González Clavijo, E., and Díez Montes, A., 2008, Procesos tardivariscos en la Zona Centro Ibérica: Las bandas de cizalla subverticales del domo de tormes. Geo-Temas, v. 10, p. 445–448.

Gutiérrez-Alonso, G., Collins, A.S., Fernández-Suárez, J., Pastor-Galán, D., González-Clavijo, E., Jourdan, F., Weil, A.B., and Johnston, S.T., 2015, Dating of lithospheric buckling: 40Ar/39Ar ages of syn-orocline strike–Slip shear zones in northwestern Iberia: Tectonophysics, v. 643, p. 44–54. doi:10.1016/j.tecto.2014.12.009

Gutiérrez-Alonso, G., Fernández-Suárez, J., Jeffries, T.E., Johnston, S.T., Pastor-Galán, D., Murphy, J.B., Franco, M.P., and Gonzalo, J.C., 2011a, Diachronous post-orogenic magmatism within a developing orocline in Iberia, European Variscides: Tectonics, v. 30, p. 17. doi:10.1029/2010TC002845

Gutiérrez-Alonso, G., Fernández-Suárez, J., and Weil, A.B., 2004, Orocline triggered lithospheric delamination, *in* Weil, A.B., and Sussman, A., eds., Special paper: Boulder, Geological Society of America, p. 121–131.

Gutiérrez-Alonso, G., Johnston, S.T., Weil, A.B., Pastor-Galán, D., and Fernández-Suárez, J., 2012, "Buckling an orogen: The Cantabrian Orocline: GSA Today, v. 22, p. 4–9. doi:10.1130/GSATG141A.1

Gutiérrez-Alonso, G., Murphy, J.B., Fernández-Suárez, J., and Hamilton, M.A., 2008, Rifting along the northern Gondwana margin and the evolution of the Rheic Ocean: A Devonian age for the El Castillo volcanic rocks (Salamanca, Central Iberian Zone): Tectonophysics, v. 461, no. P070, p. 157–165. doi:10.1016/j.tecto.2008.01.013

Gutiérrez-Alonso, G., Murphy, J.B., Fernández-Suárez, J., Weil, A.B., Franco, M.P., and Gonzalo, J.C., 2011b, Lithospheric delamination in the core of Pangea: Sm-Nd insights from the Iberian mantle: Geology, v. 39, p. 155–158. doi:10.1130/G31468.1

Gutiérrez-Marco, J.C., San José, M.A., and Pieren, A.P., 1990, Post-Cambrian Paleozoic stratigraphy, *in* Dallmeyer, R.D., and Martínez García, E., eds., Pre-Mesozoic Geology of Iberia: Germany, Springer-Verlag, p. 160–171.

Li, P., and Rosenbaum, G., 2014, Does the manning Orocline exist? New structural evidence from the inner hinge of the Manning Orocline (eastern Australia): Gondwana Research, v. 25, p. 1599–1613. doi:10.1016/j.gr.2013.06.010

López-Carmona, A., Abati, J., Pitra, P., and Lee, J.K.W., 2014, Retrogressed lawsonite blueschists from the NW Iberian Massif: P–T–t constraints from thermodynamic modelling and 40Ar/39Ar geochronology: Contributions to Mineral Petrol, v. 167, p. 987. doi:10.1007/s00410-014-0987-5

López-Moro, F.J., López-Plaza, M., and Romer, R.L., 2012, Generation and emplacement of shear-related highly mobile crustal melts: The synkinematic leucogranites from the Variscan Tormes Dome, Western Spain: International Journal of Earth Sciences, v. 101, p. 1273–1298. doi:10.1007/s00531-011-0728-1

Martínez Catalán, J.R., 2011, Are the oroclines of the Variscan belt related to late Variscan strike-slip tectonics?: Terra, Nov, v. 23, p. 241–247. doi:10.1111/j.1365-3121.2011.01005.x

Martinez Catalán, J.R., Aerden, D.G., and Carreras, J., 2015. The "castilian bend" of rudolf staub (1926): historical perspective of a forgotten orocline in central iberia. Swiss Journal Of Geosciences, 108(2–3), pp.289–303.

Martinez Catalan, J.R., Rubio Pascual, F.J., Diez Montes, A., Diez Fernandez, R., Gomez Barreiro, J., Dias da Silva, I., Gonzalez Clavijo, E., Ayarza, P., Alcock, J.E., Montes, A.D., Fernandez, R.D., Barreiro, J.G., Dias da Silva, I., Clavijo, E.G., Ayarza, P., and Alcock, J.E., 2014, The late Variscan HT/LP metamorphic event in NW and Central Iberia: Relationships to crustal thickening, extension, orocline development and crustal evolution: Geological Social London, Special Publication, v. 405, p. 225–247. doi:10.1144/SP405.1

Martínez-Catalán, J.R., 1990, A non-cylindrical model for the northwest Iberian allochthonous terranes and their equivalents in the Hercynian belt of Western Europe: Tectonophysics, v. 179, p. 253–272. doi:10.1016/0040-1951(90)90293-H

Meijers, M.J.M., Smith, B., Pastor-Galán, D., *Degenaar, R., Sadradze, N., Adamia, S., Sahakyan, L., Avagyan, A., Sosson, M., Rolland, Y., Langereis, C.G., and Müller, C., 2017, Progressive orocline formation in the Lesser Caucasus as a result of South Armenian Block – Eurasia collision: Special Publication of Journal of the Geological Society, v. 428, p. 117–143. doi:10.1144/SP428.8

Mulchrone, K.F.K.F., Pastor-Galán, D., and Gutiérrez-Alonso, G., 2013, Mathematica code for least-squares cone fitting equal-area stereonet representation: Computational Geoscience, v. 54, p. 203–210. doi:10.1016/j.cageo.2013.01.005

Murphy, J.B., Quesada, C., Gutiérrez-Alonso, G., Weil, A.B., and Johnston, S.T., 2016, Reconciling competing models for the Tectono-Stratigraphic zonation of the Variscan Orogen in Western Europe: Tectonophysics, v. 681, p. 209–219. (P134). doi:10.1016/j.tecto.2016.01.006

Nance, R.D., Gutiérrez-Alonso, G., Keppie, J.D., Linnemann, U., Murphy, J.B., Quesada, C., Strachan, R.A., and Woodcock, N. H., 2010, Evolution of the Rheic Ocean: Gondwana Researcher, v. 17, p. 194–222. doi:10.1016/j.gr.2009.08.001

Pastor-Galán, D., Dekkers, M.J., Gutiérrez-Alonso, G., Brouwer, D., Groenewegen, T., Krijgsman, W., Fernández-Lozano, J., Yenes, M., and Álvarez-Lobato, F., 2016, Paleomagnetism of the Central Iberian curve's putative hinge: Too many oroclines in the Iberian Variscides: Gondwana Researcher, v. 39, p. 96–113. doi:10.1016/j.gr.2016.06.016

Pastor-Galán, D., Groenewegen, T., Brouwer, D., Krijgsman, W., and Dekkers, M.J., 2015b, One or two oroclines in the Variscan orogen of Iberia? Implications for Pangea amalgamation: Geology, v. 43, p. 527–530. doi:10.1130/G36701.1

Pastor-Galán, D., Gutiérrez-Alonso, G., Langereis, C.G., and Dekkers, M., Paleomagnetism in Extremadura (Central Iberian Zone, Spain), in press, Paleozoic rocks: Extensive remagnetizations and further constraints on the extent of the Cantabrian orocline: Accepted in Journal of Iberian Geology. https://doi.org/10.1007/s41513-017-0039-x

Pastor-Galán, D., Gutiérrez-Alonso, G., Meere, P.A., and Mulchrone, K.F., 2009, Factors affecting finite strain estimation in low-grade, low-strain clastic rocks: Journal Structureal Geological, v. 31, p. 1586–1596. doi:10.1016/j.jsg.2009.08.005

Pastor-Galán, D., Gutiérrez-Alonso, G., Mulchrone, K.F., and Huerta, P., 2012b, Conical folding in the core of an orocline. A geometric analysis from the Cantabrian Arc (Variscan Belt of NW Iberia): Journal Structureal Geological, v. 39, p. 210–223. doi:10.1016/j.jsg.2012.02.010

Pastor-Galán, D., Gutiérrez-Alonso, G., and Weil, A.B., 2011, Orocline timing through joint analysis: Insights from the Ibero-Armorican Arc: Tectonophysics, v. 507, p. 31–46. doi:10.1016/j.tecto.2011.05.005

Pastor-Galan, D., Gutierrez-Alonso, G., Zulauf, G., Zanella, F., Pastor-Galán, D., and Gutiérrez-Alonso, G., 2012a, Analogue modeling of lithospheric-scale orocline buckling: Constraints on the evolution of the Iberian-Armorican Arc: Geological Social American Bulletin, v. 124, p. 1293–1309. doi:10.1130/B30640.1

Pastor-Galán, D., Martín-Merino, G., and Corrochano, D., 2014, Timing and structural evolution in the limb of an orocline: The Pisuerga–Carrión Unit (southern limb of the Cantabrian Orocline, NW Spain): Tectonophysics, v. 622, p. 110–121. doi:10.1016/j.tecto.2014.03.004

Pastor-Galán, D., Mulchrone, K.F., Koymans, M., van Hinsbergen, D.J.J., and Langereis, C.G., 2017, Bootstrapped Total Least Squares orocline test: A robust method to quantify vertical axis rotation patterns in orogens, with examples from the Cantabrian and Aegean oroclines: Lithosphere, v. 9, p. 499–511. doi:10.1130/L547.1 PDF.

Pastor-Galán, D., Ursem, B., Meere, P.A., and Langereis, C., 2015a, Extending the Cantabrian Orocline to two continents (from Gondwana to Laurussia). Paleomagnetism from South Ireland: Earth and Planetary Science Letters, v. 432, p. 223–231. doi:10.1016/j.epsl.2015.10.019

Pereira, E., 1987, Estudo geológico-estructural da região de Celorico de Basto e sua intrepretação geodinâmica: Lisboa, Universidade de Lisboa, p. 274.

Pueyo, E.L., Parés, J., Millán, H., Pocoví, A., Pares, J.M., Millan, H., and Pocovi, A., 2003, Conical folds and apparent rotations in paleomagnetism (a case study in the Southern Pyrenees): Tectonophysics, v. 362, p. 345–366. doi:10.1016/S0040-1951(02)00645-5

Quesada, C., 1991, Geological constraints on the Paleozoic tectonic evolution of tectonostratigraphic terranes in the Iberian Massif: Tectonophysics, v. 185, p. 225–245. doi:10.1016/0040-1951(91)90446-Y

Ramsay, J.G., 1967, Folding and fracturing of rocks (First Edit ed): McGraw-Hill Book Company, New York.

Ribeiro, A., 1974, Contribution à l'étude tectonique de Trás-os-Montes Oriental: Memory Services Geological Portugal, v. 24, p. 168.

Ribeiro, A., Pereira, E., and Dias, R., 1990, Allochtonous sequences – Structure in the Northwest of the Iberian Peninsula., *in* Dallmeyer, R.D., and Martínez García, E., eds., Pre-Mesozoic Geology of Iberia: Germany, Springer-Verlag, p. 222–236.

Rodrigues, J.F., Ribeiro, A., and Pereira, E., 2013, Complexo de Mantos Parautóctones do NE de Portugal: Estructurainterna e tectonoestratigrafia, *in* Dias, R., Araújo, A., Terrinha, P., and Kullberg, J.C., eds., Lisboa: Geologia de Portugal, p. 275–331.

Rubio Pascual, F.J., Arenas, R., Martínez Catalán, J.R., Rodríguez Fernández, L.R., and Wijbrans, J.R., 2013, Thickening and exhumation of the Variscan roots in the Iberian Central System: Tectonothermal processes and 40Ar/39Ar ages: Tectonophysics, v. 587, p. 207–221. doi:10.1016/j.tecto.2012.10.005

Rubio Pascual, F.J., López-Carmona, A., and Arenas, R., 2016, Thickening vs. extension in the Variscan belt: P–T modelling in the Central Iberian autochthon: Tectonophysics, v. 681, p. 144–158. doi:10.1016/j.tecto.2016.02.033

Shaw, J., Gutierrez-Alonso, G., Johnston, S.T., Galan, D.P., and Pastor Galan, D., 2014, Provenance variability along the Early Ordovician north Gondwana margin: Paleogeographic and tectonic implications of U-Pb detrital zircon ages from the Armorican Quartzite of the Iberian Variscan belt: Geological Social American Bulletin, v. 126, p. 702–719. doi:10.1130/B30935.1

Shaw, J., and Johnston, S.T., 2016b, Terrane wrecks (coupled oroclines) and paleomagnetic inclination anomalies: Earth-Science Reviews, v. 154, p. 191–209. doi:10.1016/j.earscirev.2016.01.003

Shaw, J., Johnston, S.T., and Gutiérrez-Alonso, G., 2016a, Orocline formation at the core of Pangea: A structural study of the Cantabrian orocline, NW Iberian Massif: Lithosphere, v. 8, p. 97.

Shaw, J., Johnston, S.T., Gutiérrez-Alonso, G., and Weil, A.B., 2012, Oroclines of the Variscan orogen of Iberia: Paleocurrent analysis and paleogeographic implications: Earth and Planetary Science Letters, v. 329–330, p. 60–70. doi:10.1016/j.epsl.2012.02.014

Stampfli, G.M., Hochard, C., Vérard, C., Wilhem, C., and VonRaumer, J., 2013, The Formation of Pangea: Tectonophysics, v. 593, p. 1–19. doi:10.1016/j.tecto.2013.02.037

Staub, R., 1926, Gedanken zur Tektonik Spaniens., Vierteljahrss- chrift der Naturforschenden Gesellschaft: Zürich.Naturforschende Gesellschaft.

Valladares, M.I., Barba, P., Ugidos, J.M., Colmenero, J.R., and Armenteros, I., 2000, Upper Neoproterozoic–Lower Cambrian sedimentary successions in the Central Iberian Zone (Spain): Sequence stratigraphy, petrology and chemostratigraphy. Implications for Other European Zones: International Journal of Earth Sciences, v. 89, p. 2–20. doi:10.1007/s005310050314

van Der Boon, A., Gürer, D., van Hinsbergen, D.J.J., Pastor-Galán, D., Rezaeian, M., Honarmand, M., Krijgsman, W., and Langereis, C.G., 2018, Quantifying Arabia–Eurasia convergence accommodated in the Greater Caucasus by paleomagnetic reconstruction: Epsl, v. 482, p. 454–469. doi:10.1016/j.epsl.2017.11.025

Weil, A., Gutiérrez-Alonso, G., and Conan, J., 2010, New time constraints on lithospheric scale oroclinal buckling of the Ibero-Armorican arc: A palaeomagnetic study of earliest Permian rocks from Iberia: Journal of the Geological Society of London, v. 167, p. 127–143. doi:10.1144/0016-76492009-002

Weil, A.B., Gutiérrez-Alonso, G., Johnston, S.T., and Pastor-Galán, D., 2013, Kinematic constraints on buckling a lithospheric-scale orocline along the northern margin of Gondwana: A geologic synthesis: Tectonophysics, v. 582, p. 25–49. doi:10.1016/j.tecto.2012.10.006

Wu, S., 1993, Fractal strain distribution and its implications for cross-section balancing: Journal Structureal Geological, v. 15, p. 1507–1993. doi:10.1016/0191-8141(93)90009-Y